Astron. Astrophys. 353, 311–321 (2000)

ASTRONOMY AND ASTROPHYSICS

An exploratory non-LTE analysis of B-type supergiants in the Small Magellanic Cloud

P.L. Dufton[1,⋆], **N.D. McErlean**[1], **D.J. Lennon**[2], **and R.S.I. Ryans**[1]

[1] The Department of Pure and Applied Physics, The Queen's University of Belfast, Belfast BT7 1NN, Ireland
[2] Isaac Newton Group of Telescopes, Apartado de Correos 368, 38700 Santa Cruz de La Palma, Canary Islands, Spain

Received 2 July 1999 / Accepted 8 October 1999

Abstract. A preliminary differential non-LTE model atmosphere analysis of moderate resolution ($R \sim 5\,000$) and signal-to-noise ratio spectra of 48 Small Magellanic Cloud B-type supergiants is presented. Standard techniques are adopted, viz. plane-parallel geometry and radiative and hydrostatic equilibrium. Spectroscopic atmospheric parameters ($T_{\rm eff}$, $\log g$ and $v_{\rm turb}$), luminosities and chemical abundances (He, C, N, O, Mg and Si) are estimated.

These are compared with those deduced for a comparable sample of Galactic supergiants. The SMC targets appear to have similar atmospheric parameters, luminosities and helium abundances to the Galactic sample. Their magnesium and silicon underabundances are compatible with those found for main sequence SMC objects and there is no evidence for any large variation in their oxygen abundances. By contrast both their carbon and nitrogen lines strengths are inconsistent with single abundances, while their nitrogen to carbon abundance ratios appear to vary by at least as much and probably more than that found in the Galactic sample.

Key words: stars: atmospheres – stars: early-type – stars: evolution – stars: supergiants – galaxies: abundances – galaxies: Magellanic Clouds

1. Introduction

The Large (LMC) and Small (SMC) Magellanic Clouds are two irregular galaxies which are satellites to our own Galaxy. Abundance analyses of their early-type stellar populations (see, for example, Rolleston et al. 1993, 1996 for main sequence B-type stars and Venn et al. 1998 for A-type supergiants) have found metal depletions of the order of -0.3 and -0.8 dex for the LMC and SMC respectively. The uniformity of these depletions with respect to chemical species or position is still subject to debate (Lennon et al. 1996, Rolleston et al. 1993). Nevertheless, both from early-type stellar and other studies (see, for example, Hill 1998), the LMC is clearly metal weak relative to our local Galactic environment, with the SMC being even more depleted in metals. These galaxies, therefore, constitute unique astrophysical laboratories; their reduced metallicities, coupled with their small internal and foreground extinctions, allow their entire massive star populations to be observed and the effects of metallicity on both spectral morphology and stellar evolution to be investigated.

As well as the uncertainties connected with such processes as convection, mass loss and stellar rotation (see, for example Maeder & Meynet 1989, Denissenkov 1994, Talon et al. 1997), stellar evolutionary computations are sensitive to the initial metallicity, z. For example, the efficiency of chemical mixing (by whatever mechanism), the position and extent of the main sequence, the size of any blue loops and the ratio of blue to red supergiants within a stellar sample are all functions of metallicity (see, for example, Schaller et al. 1992, Langer & Maeder 1995). Venn (1995a, 1995b, 1999) and Venn et al. (1998) have examined and compared the evolutionary histories (and in particular the chemical mixing) for both Galactic and SMC A-type supergiants. For the Galactic targets, Venn (1995b) showed that mixing of CN-processed material had occurred but that the abundances had changed by less than that predicted for the post first dredge-up. This implied that mixing had occurred during the main sequence lifetime and also that they were pre-RSG supergiants. The subsequent analyses of more luminous SMC A-type supergiants (Venn et al. 1998, Venn 1999) revealed a greater degree of chemical mixing in their atmospheres, which could be caused by either more efficient rotational mixing during the main sequence or by a blue loop evolutionary history. Indeed the variation in nitrogen abundances imply that rotational mixing has taken place but Venn (1999) concludes that 'the overall overabundance of nitrogen in the sampled stars implies these stars have undergone the first dredge-up in addition to having been mixed while on the main-sequence'.

Hence, despite the success of recent stellar evolutionary models which include rotation (see for example, Langer & Heger 1998, Meynet 1998), the blue loop evolutionary history may still be appropriate in some cases. Indeed for Sk -69° 202, the B-type supergiant progenitor of SN1987A in the LMC, an analysis of IUE nebular emission lines by Fransson et al. (1989) has shown that circumstellar material has abundance patterns appropriate to CNO-processed material. These emission lines

Send offprint requests to: P.L. Dufton (P.Dufton@qub.ac.uk)

⋆ On leave of absence at the Isaac Newton Group of Telescopes, Apartado de Correos 368, E-38700, Santa Cruz de La Palma, Canary Islands, Spain

are so strong that a fast stellar wind must be causing shocks as it 'catches up' with a slow wind and hence they conclude that Sk -69° 202 (a B3 supergiant) had a RSG evolutionary stage some 10^4 years prior to its explosion.

Recently, we have undertaken a non-LTE model atmosphere analysis of 46 Galactic B-type supergiants (McErlean et al. 1999; hereafter MLD). We identified a group of stars with near normal chemical compositions which may be following an analogous evolutionary history to the Galactic A-type supergiant sample of Venn (1995b). Two other groups of higher mass supergiants (in different effective temperature regimes) were also identified with atmospheres that appeared to contain significant amounts of nuclear processed material. Whether this reflected different amounts of mixing on the main sequence (due to their larger masses or rotational velocities) or whether they were the product of binary evolution (see, for example, Langer et al. 1999) was unclear.

Here we undertake a similar study for a sample of SMC supergiants. The principal motivations were — firstly to attempt to quantify the abundance depletions of the SMC supergiants relative to our Galactic sample using reliable and consistent techniques — secondly to examine the evidence for CNO-processed matter in the SMC supergiants' atmospheres, with a view to clarifying their evolutionary histories and in particular whether at least some of them may be at a post-RSG evolutionary stage — thirdly to identify normal and nuclear processed targets for further higher resolution specroscopy.

2. Observational data

The SMC supergiant sample has been previously discussed by Lennon (1997) and below, we briefly summarize his target selection and observational setup; further details can be found in Lennon (1997).

A subset of the brightest B0-B9 supergiants in the SMC, taken from the compilation of Garmany et al. (1987), were selected. Particular emphasis was placed on the earlier spectral types in order to investigate the behaviour of the important CNO lines. Spectra were obtained at La Silla, Chile using the ESO NTT and the EMMI instrument operated by remote control from Garching in Germany. Data were acquired during two observing runs, on October 7^{th} 1993 and October 22^{nd}-24^{th} 1994, using gratings #3 and #6 in the blue and red arms respectively. For both observing runs the ESO CCD#31 (Tektronix TK 1024 AB) was used in the blue arm, while during the second run the ESO CCD#36 (Tektronix TK 2048) was used in the red arm. Both CCDs have a pixel size of 24 μm which resulted in dispersions of approximately 0.45 Å per pixel in the blue and 0.32 Å per pixel in the red. For a $1''$ slit (used throughout) this gave FWHM resolutions of 1.18 Å, 1.27 Å and 1.21 Å at Hα, Hγ and Hδ respectively. Each star was observed in three wavelength regions; in one exposure the dichroic was used to simultaneously obtain data in the blue and red arms covering the approximate wavelength regions 3925–4375 Å and 6190–6830 Å, and another exposure in the blue arm covered the region 4300–4750 Å. Exposure times depended on conditions and the visual magnitude of the target but were typically 10 to 15 minutes giving a signal-to-noise ratio normally in excess of 70.

Table 1 contains the complete list of targets, ordered by their number in the stellar catalogue of Azzopardi & Vigneau (1982), their aliases in the catalogue of Sanduleak (1968), their photometric data (Azzopardi & Vigneau 1982, Garmany et al. 1987) and their spectral types, as estimated by Lennon (1997).

3. Model atmosphere calculations

The model atmosphere techniques have been desribed in detail by MLD and here we only provide a summary. A grid of non-LTE model atmospheres was generated using the code TLUSTY (Hubeny 1988) for effective temperatures, 10 000 K $\leq T_{\rm eff} \leq$ 35 000 K and logarithmic gravities from $\log g = 4.5$ down to near the Eddington stability limit. Models were calculated for two helium fractions, viz. y = 0.09 (solar) and y = 0.20, where y=N[He]/N[H+He]. The models omit a number of physical processes, including metal line-blanketing and wind-blanketing. Given the lower metallicity of the the SMC, the importance of these processes are likely to be smaller than for our galactic sample. Furthermore, the assumption of a plane-parallel geometry may be of limited validity for the low gravity objects considered here. The consequences of these omissions have been discussed in MLD.

The line formation calculations were performed using the codes DETAIL and SURFACE (Giddings 1981 and Butler 1984 respectively). Microturbulent velocities, which are close to the speed of sound, have been found for B-type supergiants. Therefore, in the calculation of line profiles, microturbulence has been included as an extra free parameter. Metal ion populations and line-profiles were calculated using mainly the atomic data of Becker & Butler (1988, 1989, 1990 and references therein).

Significant difficulties were encountered in running DETAIL particularly for the silicon model ion but also for some other species. These difficulties occured mainly at the lowest gravities for effective temperatures greater than $\sim$ 25 000 K. Examination of the line profiles indicated that this was caused by either emission or 'filling in' of the profiles. Indeed the DETAIL calculations normally showed an overpopulation of the relevant ionic upper levels coupled with large photoionisation rates (and subsequent cascades). MLD postulated that the emission was an artefact of their exclusion of line blanketing which leads to an overestimate of the UV flux and hence of the photoionisation rates - further discussion of these problems can again be found in MLD, while their implications for the current dataset are discussed below.

4. Estimation of atmospheric parameters

In order to compare results for the Galactic and the SMC supergiants, it is important that their atmospheric parameters are assigned consistently. There are a number of indicators which could potentially be used for the SMC sample and these are discussed below. Note that again further details can be found in MLD.

Table 1. Small Magellanic Cloud supergiants and associated data. Stellar identification numbers are from Azzopardi & Vigneau (1982; AV#) and Sanduleak (1968; Sk#). V-magnitudes and colours are taken from Azzopardi & Vigneau, except for those objects marked with a dagger, whose photometric data are taken from Garmany et al. (1987). The spectral types are from Lennon (1997) and AV 415 is a Luminous Blue Variable, whose spectral type from these data is somewhat uncertain. The luminosities were estimated as discussed in Sect. 5.2.

AV #	Sk #	V	B-V	E(B-V)	$\log\frac{L}{L_\odot}$	Sp. Type	AV #	Sk #	V	B-V	E(B-V)	$\log\frac{L}{L_\odot}$	Sp. Type
2	3	11.99	+0.04	0.06	5.05	B8 Ia$^+$	264	94	12.36	−0.15	0.05	5.38	B1 Ia
6	–	13.46	+0.03	0.33	5.71	O9 III	268	96	13.14	−0.13	0.05	4.86	B2.5 Iab
10	7	12.64	−0.06	0.08	5.10	B2.5 Ia	270	98	11.42	+0.03	0.05	5.09	A0 Ia
18	13	12.46	+0.03	0.18	5.38	B2 Ia	271	–	13.46	−0.16	0.05	4.89	B1.5 Iab
22	15	12.25	−0.10	0.05	5.07	B5 Ia	297	–	12.18	−0.06	0.05	4.95	B8 Ia
23	17	12.25	+0.07	0.21	5.36	B3 Ia	303	–	12.81	−0.13	0.05	5.15	B1.5 Iab
48	27	11.03	−0.02	0.07	5.58	B5 Ia	314	–	12.90	−0.12	0.05	4.81	B5 Iab
56	31	11.15	0.00	0.14	5.77	B2.5 Ia	315	106	10.90	+0.06	0.06	5.31	A0 Ia
65	33	11.03	+0.12	0.15	5.53	B8 Ia$^+$	320	–	12.94	−0.17	0.05	4.88	B3 Iab
76	39	11.19	+0.12	0.11	5.36	B9 Ia$^+$	337	–	12.78	−0.11	0.05	5.09	B2 Iab
78	40	11.09	−0.02	0.13	5.95	B1.5 Ia$^+$	340	–	12.71	−0.06	0.11	5.31	B1 Ia
86	42	12.83	−0.16	0.05	5.19	B1 Ia	342	–	12.59	−0.03	0.11	5.16	B2.5 Iab
96	46	12.62	−0.14	0.05	5.23	B1.5 Ia	362	114	11.36	−0.03	0.09	5.57	B3 Ia
97	–	13.30	−0.12	0.05	4.88	B2 Iab	367	117	11.22	+0.07	0.07	5.28	B9 Ia$^+$
98	45	11.49	+0.04	0.05	5.06	A0 Ia	373	119	12.17	−0.09	0.06	5.34	B2 Ia
99	–	13.01	−0.09	0.05	4.92	B2.5 Iab	374	–	13.11	−0.17	0.05	4.96	B2 Ib
101	47	12.14	+0.07	0.08	4.94	B9 Ia	382	121	11.41	+0.06	0.05	5.10	A0 Ia
103	–	13.36	−0.12	0.06	5.03	B0.7 Ib	404	128	12.20	−0.12	0.05	5.24	B2.5 Iab
104	–	13.13	−0.22	0.05	5.16	B0.5 Ia	415	130	10.52	+0.10	0.11	5.57	A2 Ia: (LBV)
125	52	12.56	+0.05	0.17	5.19	B3 Ia	420	131	13.14	−0.24	0.05	5.15	B0.5 Ia
137	53	12.42	−0.06	0.09	5.28	B2 Iab	443	137	10.98	−0.08	0.08	5.77	B2.5 Ia
151	57	12.30	−0.06	0.08	5.24	B2.5 Ia	445	138	12.78	−0.10	0.05	4.85	B5 Iab
173	62	12.76	−0.08	0.08	5.21	B1.5 Ia	462	145	12.56	−0.17	0.05	5.24	B1.5 Ia
187	68	12.09	−0.13	0.05	5.22	B3 Ia	472	150	12.65	−0.14	0.05	5.14	B2 Ia
200	69	12.10	+0.07	0.10	5.04	B8 Ia	479	155	12.48	−0.15	0.15	5.88	O9 Ib
210	73	12.67	−0.05	0.11	5.28	B1.5 Ia	487	158	12.70	−0.17	0.05	5.44	BC0 Ia
215	76	12.77	−0.11	0.07	5.44	BN0 Ia	490	160	13.21	−0.16	0.13	5.52	O9.5 II
242	85	12.11	−0.13	0.05	5.48	B1 Ia	504	168	11.91	−0.03	0.05	5.00	B9 Ia
252	87	13.07	−0.10	0.05	4.89	B2.5 Iab	–	56	10.87	+0.04†	0.07	5.50	B8 Ia$^+$
257	91	12.79	−0.07	0.07	5.03	B2.5 Iab	–	191	11.86	−0.04†	0.12	5.62	B1.5 Ia
260	92	13.28	−0.17	0.05	4.96	B1.5 Iab	–	196	12.04	−0.02†	0.05	5.00	B8 Ia
263	93	12.85	+0.00	0.05	4.64	B9 Ia	–	202	12.32	−0.09†	0.05	5.04	B5 Iab

Balmer lines profiles: These can be used to constrain the gravity. The Hδ and Hγ line profiles were observed in both our samples, allowing a consistent application of this method. Additionally as was previously found by MLD for the Galactic sample, the agreement between the two lines was generally good for the SMC supergiants.

He II profile fits: As for the Galactic sample, the He II lines at 4542 & 4200 Å were used to provide estimates of effective temperature with He II 4686 Å again not being used as it is affected by the stellar wind (Gabler et al. 1989). However, only the six hottest SMC supergiants had spectra with well-observed He II line profiles.

Silicon ionisation balances: Ionisation balances due to Si II/III or Si III/IV provided the bulk of the $T_{\rm eff}$-scale for the Galactic supergiants, but the intrinsic weakness of the metal lines meant that only *four* SMC B5-type supergiants showed lines due to two ionisation stages simultaneously, namely AV 22, AV 445, AV 314 and Sk202 (for the other B5 supergiant, AV 22, it was only possible to set upper limits on the Si III line strengths). For the first two stars, the Si II doublet near 4130 Åwas badly blended and it was not possible to measure reliable equivalent.

Hence, by using these three indicators, atmospheric parameters ($T_{\rm eff}$ and $\log g$) have been estimated for eight of the 64 SMC supergiants and these are listed in Table 2.

Other possible temperature diagnostics include:

Continuum fitting of low resolution IUE spectra. For example, Rolleston et al. (1993, 1996) used this method to estimate effective temperatures for their main sequence Magellanic Cloud stars. However, as the ultraviolet spectral region is dominated by metal absorption lines, a fit using the unblanketed non-LTE continua would be unrealistic. Furthermore, to use the blanketed LTE model fluxes of Kurucz (1991), as used by Rolleston et al., would yield estimates which would be inconsistent with the Galactic study, as discussed by MLD

Strömgren photometry. The Strömgren reddening-free indices, $[c_1]$ and $[u-b]$ have also been used to assign temperatures to main sequence B-type stars (see, e.g., Rolleston et al. 1993). However their application to supergiant stars is problematic for

a number of reasons. In particular, the low gravities mean that extrapolations from the published colour grids (e.g. Lester et al. 1986) are required, while the indices are not particularly sensitive to temperature in this gravity regime. Also, the colours are normally calibrated using main sequence objects – Lester et al. used only main sequence stars to calibrate their colour grid and include only one B-type star, η UMa (B3 V). Hence these grids may be unsuitable for supergiants and in any case would be on an LTE line blanketed scale and again incompatible with our Galactic sample.

We have therefore not attempted to use these methods but have instead assigned effective temperatures on the basis of spectral type. The previous study by Lennon (1997) of our targets shows that the different metallicity between the local Galactic environment and the SMC leads to striking changes in their visible spectral morphology. Metal line strengths are dramatically reduced leading to difficulties for a spectral type classification scheme and its applicability across a range of metallicities. In fact, for B-type visible spectra the classification process must be 3-dimensional, treating the parameters effective temperature, luminosity and also metallicity. This extension of the standard MK spectral typing procedure was considered by Walborn (1977, 1983) when he used the He I/II reference frame to classify B0 supergiants in the SMC using their visible spectra and found an inconsistency with the silicon reference frame. In spite of this, numerous spectroscopic surveys are available which have not included this important effect (e.g. Azzopardi & Vigneau 1982 and Humphreys 1983).

Hence, for the early B-type supergiants whose spectra show absorption features due to He II, spectral typing consistent with equivalent Galactic objects is relatively straightforward. However, new methods are required in order to assign spectral types to mid and late B-type supergiants. Lennon (1997) used the Balmer lines as luminosity indicators and ratios of lines strengths due to Si II/III/IV, Mg II and He I as temperature indicators, with approximately 75 % of the supergiants requiring new spectral types. A subsequent mapping of his spectral bins onto the MK scale led to a significant improvement over previous work in terms of consistency, with for example the observational HR diagram now being comptaible with its galactic counterpart.

The validity of using the spectral types of Lennon (1997) can be checked by comparing the effective temperatures derived for the eight SMC supergiants given in Table 2 with those for Galactic supergiants of similar spectral types (see Table 3). The latter were compiled from the estimates in MLD and are, for the most part, simple averages of the effective temperatures of the Ia supergiants at each spectral type. The agreement is generally good and furthermore, the He II temperature at ∼B0 and the Si II/III temperature at B5 provide anchor points which imply that the Galactic and SMC $T_{\rm eff}$-spectral type scales are similar between these two spectral types (where the important CNO lines are strong). Therefore, the values given in Table 3 were *adopted* for all the SMC supergiants, with the 15 objects later than B5 excluded from the analysis, thereby reducing our sample to 48 targets.

Table 2. SMC supergiants and their non-LTE atmospheric parameters. Note that the effective temperatures and logarithmic gravities are the associated non-LTE model parameters and that they may not be physically realistic.

AV/Sk number	Spectral Type	$T_{\rm eff}$ (K)	$\log g$
6	O9 III	35 000[1]	3.75
479	O9 Ib	34 000[1]	3.30
490	O9.5 II	30 000[1]	3.15
215	BN0 Ia	27 500[1]	2.90
487	BC0 Ia	27 500[1]	3.00
104	B0.5 Ia	27 500[1]	3.10
314	B5 Iab	16 000[2]	2.30
202	B5 Iab	16 000[2]	2.25

Effective temperatures deduced from
[1] He II profile fits
[2] Si II/Si III ionisation balance

Table 3. The effective temperatures *adopted* for the SMC supergiants, based upon the Galactic estimates. Again, the values are likely to represent model parameters and may not be physically realistic.

Sp. Type	$T_{\rm eff}$/K
O9	34 000
O9.5	32 500
B0	28 500
B0.5	27 000
B0.7	25 500
B1	23 500
B1.5	21 500
B2	19 500
B2.5	18 500
B3	18 000
B5	15 500

Such an approach is simplistic and certainly inferior to the assignment of individual stellar atmospheric parameters which was performed for the Galactic sample, but the quality of the observational data coupled with the intrinsic weakness of the metal line spectra offers no viable alternative. Assuming that the spectral type classification is accurate to one spectral subtype, the fractional random errors in the effective temperature would range from approximately 20% at B0 spectral type to 10% at B5 spectral type. Additionally the observational errors in the hydrogen line profiles would imply that errors in the determination of the logarithmic gravity would be typically ± 0.2 dex. As well as these random errors, there may be systematic errors due to, for example, assumptions in the model atmospheric calculations. These are difficult to quantify but should be (at least) partially suppressed when making comparisons with the results of MLD for the Galactic sample.

4.1. The microturbulent velocity, $v_{\rm turb}$

The microturbulent velocity was deduced from the lines of Si III (4552, 4567, 4574 Å) for three representative SMC B-type supergiants – AV 340 (B1 Ia), AV 374 (B2 Iab) and AV 404

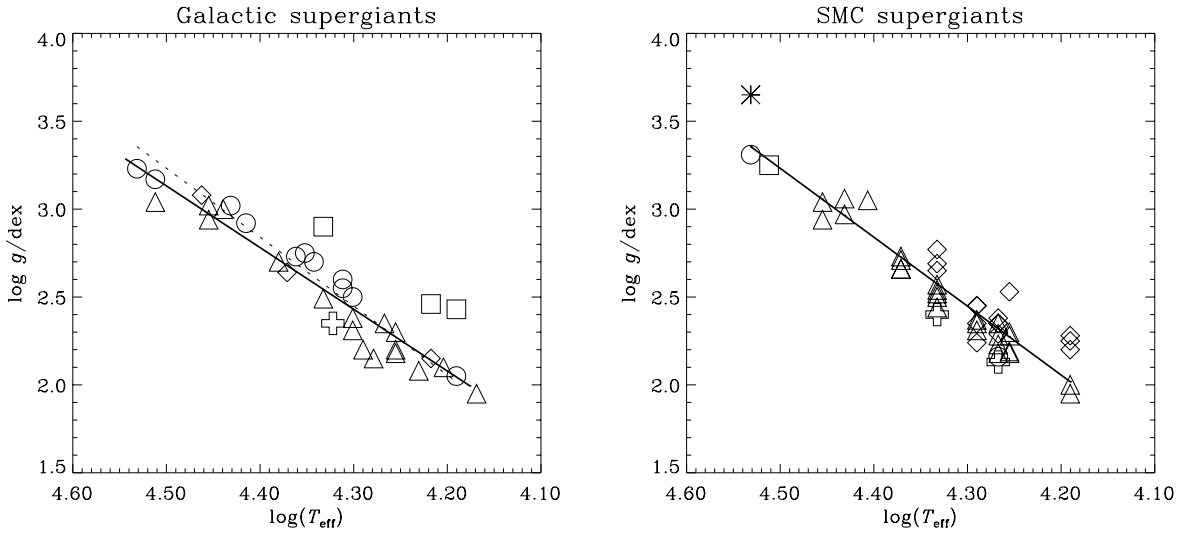

Fig. 1. *Left:* The estimated values of effective temperature and logarithmic gravity for the Galactic supergiants derived by MLD. The symbols refer to the luminosity class as follows: $+$ – Ia$^+$, $\triangle$ – Ia, $\diamond$ – Iab, $\circ$ – Ib, $\square$ – II and $*$ – III. Also shown is a linear fit (solid), which excludes the luminosity class II and III objects. This fit then represents the *average* atmospheric parameters of the more luminous supergiant sample. *Right:* The *adopted* $T_{\rm eff}$-$\log g$ values for the SMC supergiants – see text for further discussion. Again a linear fit representing the average parameters is shown. This fit is also shown in the left-hand panel (dotted) and its closeness to the Galactic fit shows that both samples may have similar atmospheric parameters.

(B2.5 Ia). This multiplet has a range of gf-values of approximately a factor of 6, which for a given star, leads to a range of equivalent widths of typically a factor of 2–3. In each of these supergiants, the range of silicon abundances was minimised for $v_{\rm turb} \sim 10\,{\rm km\,s^{-1}}$, which is in good agreement with the value adopted for the Galactic supergiants. Calculations were also undertaken for other microturbulent velocities to estimate the uncertainty. For $v_{\rm turb} = 5\,{\rm km\,s^{-1}}$, the slope in the abundance equivalent width plot was severe with the range of abundance estimates being typically 0.6 dex. For $v_{\rm turb} = 15\,{\rm km\,s^{-1}}$, variations in abundance estimates were also present but less dramatic with the range being 0.2 to 0.3 dex. Hence a conservative error estimate would be $5\,{\rm km\,s^{-1}}$ and we have adopted a uniform microturbulence of $v_{\rm turb} = 10 \pm 5\,{\rm km\,s^{-1}}$, which is consistent with that used by MLD for their Galactic sample of supergiants.

5. Results

This paper represents a preliminary attempt to determine quantitative non-LTE abundance patterns in SMC B-type supergiants and hence individual stellar analyses have not been attempted. Instead, the general behaviour of the atmospheric parameters and some representative spectral lines is examined with reference to the Galactic results.

5.1. Atmospheric parameters

Having adopted an effective temperature-spectral type calibration, individual stellar gravities were estimated from the Balmer lines. The atmospheric parameters are shown in Fig. 1 together with the equivalent Galactic plot (taken from MLD). The loci shown in this figure represent the average parameters of each sample and are reasonably consistent, with a maximum deviation of only ~ 0.1 dex in gravity at high effective temperatures. Given the methods adopted, the SMC atmospheric parameters must be considered as preliminary.

5.2. Luminosities

We have estimated luminosities for our sample assuming the distance modulus of Massey et al. (1995) and the bolometric correction – spectral type calibration of Lamers (1981). We have allowed for the effects of interstellar extinction using the reddenings listed in Table 1, which have been estimated from the intrinsic colour - spectral type calibration of Fitzpatrick (1988) and Fitzpatrick & Garmany (1990); note that when the estimated reddening was less than 0.05 magnitudes a value, E(B-V) = 0.05, has been adopted. A value of $R = A_V/(B-V)$ of 3.1 was adopted, which should be appropriate to the SMC.

In Fig. 2, luminosites are shown as a function of effective temperature for both our SMC sample and the Galactic sample of MLD. Note that for the latter, only stars with a spectral type of B5 or earlier are included to be consistent with our SMC sample. Also shown are the evolutionary tracks of Schaller et al. (1992) for metallicities appropriate to the SMC and our Galaxy. It should be noted that these tracks do not include effects due to stellar rotation or mass transfer within binary stellar systems, both of which may be important (see, MLD for further details). However assuming that they are appropriate, the principle conclusion from these figures are that the two samples are compatible covering similar ranges of luminosities ($\log L/L_\odot \sim$ 4.5–6.0) and hence stellar masses($M/M_\odot \sim$ 15–60). The only

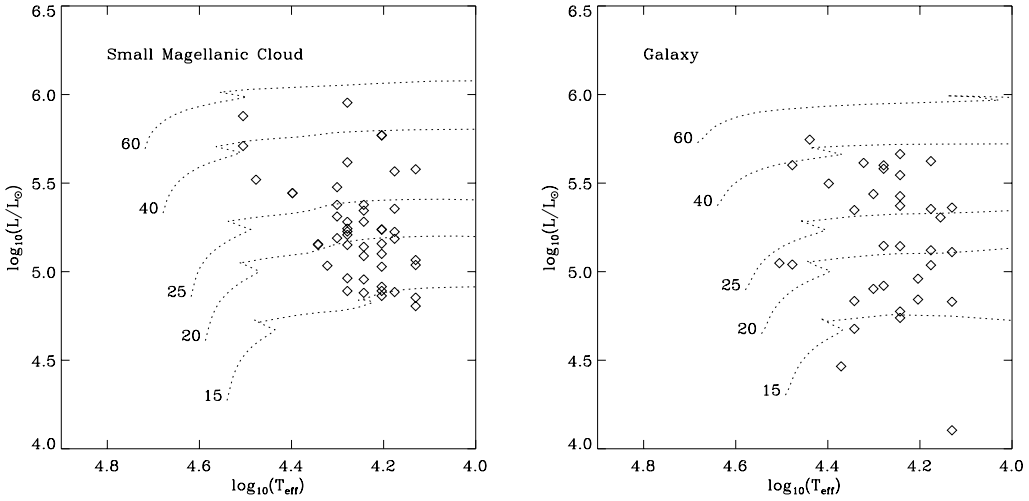

Fig. 2. The plot on the left shows luminosities as a function of effective temperature for our SMC sample, whilst the right hand graph is for the Galactic sample of MLD. In both cases only targets with a spectral type of B5 or earlier are included.

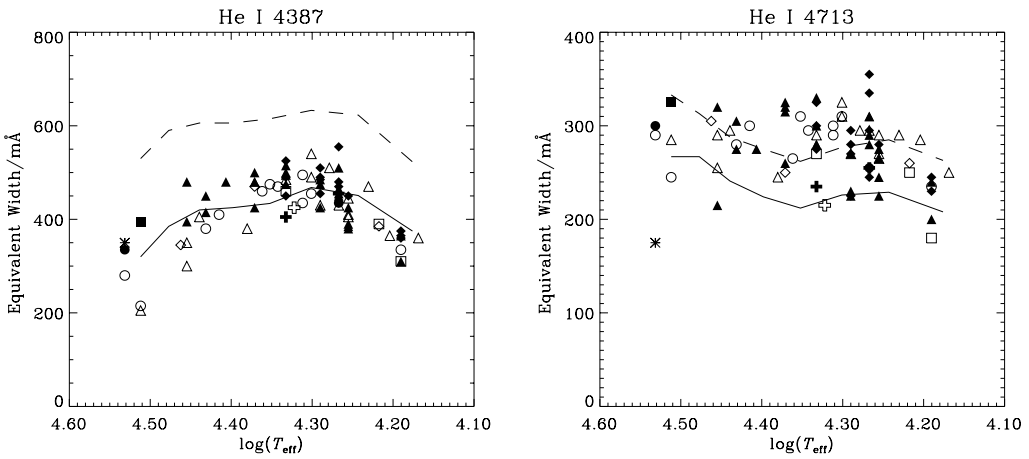

Fig. 3. Observed He I linestrengths in the Galaxy and the SMC. The plot on the left shows the He I line at 4387 Å (singlet), while that on the right shows the line at 4713 Å (triplet). The non-LTE loci are for helium fractions, $y = 0.09$ (solid lines) and $y = 0.20$ (dashed lines) and $v_{\rm turb} = 10\,{\rm km s}^{-1}$. The symbols are the same as those in Fig. 1, with the open and filled symbols representing Galactic and SMC supergiants, respectively.

significant difference may be that a greater number of Galactic supergiants lie near to the main sequence, which reflects the inclusion of fainter Ib-type objects in this sample.

5.3. Helium fractions, y

In Fig. 3, equivalent widths for two He I lines at 4387 & 4713 Å are shown for the Galactic and SMC supergiants, together with non-LTE predictions for helium fractions, $y = 0.09, 0.20$ and for $v_{\rm turb} = 10\,{\rm km\,s}^{-1}$. For the theoretical calculations, the effective temperature-gravity loci in Fig. 1 were used – hence they represent the average behaviour of the samples and do not allow for variations in gravity from these mean relationships. The singlet feature (at 4387 Å) indicates a near-normal helium fraction, whilst the triplet feature (at 4713 Å) suggests a slight helium enrichment. MLD found a similar discrepancy for their sample of galactic supergiants and attributed it to the 'generalised dilution effect' discussed by Voels et al. (1989). Voels et al. postulated that the He I level populations are enhanced due to sphericity, leading to a strengthening of the triplet lines relative to the singlets. Voels et al. also suggested that the He I singlet lines formed deepest in the atmosphere should be least affected. Hence the singlet feature at 4387 Å should provide the more reliable helium abundance estimate (see MLD for further details).

Thus, it is concluded that the SMC supergiant sample (earlier than B5 spectral type) has a near-normal helium fraction. As was the case for the Galactic sample, the observed range in linestrengths are compatible with some variation in y-value within the SMC sample. However, as the analysis used here does not account for the gravity-dependence of linestrength, this is difficult to quantify. There may also be some tentative evidence for a helium enrichment of the SMC supergiants relative to the Galactic sample at high effective temperature. These SMC supergiants lie on evolutionary tracks with larger masses (and hence luminosities) than most of our sample; a helium overabundances could imply greater mixing in the more massive SMC stars than in their galactic counterparts. However we stress that any helium enhancement is modest and may just just be an artifact of the observational and theoretical uncertainties.

5.4. Absolute metal abundances

As was the case for the Galactic supergiant sample, elemental abundances will not be estimated for any individual stars. Instead, an attempt will be made to reproduce the general be-

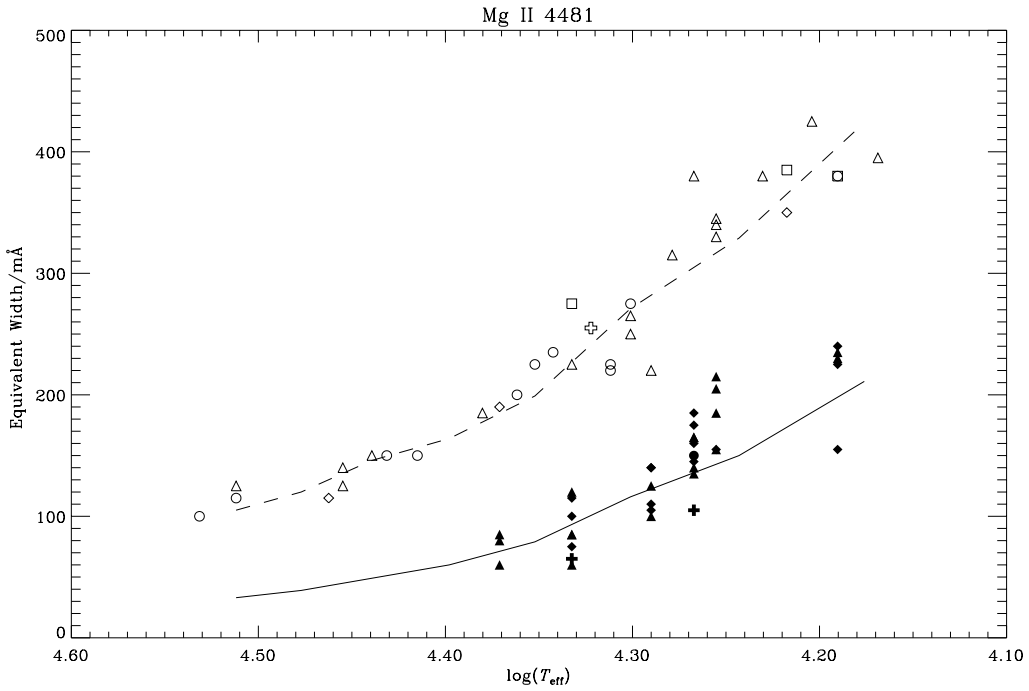

Fig. 4. Observed Mg II 4481 Å linestrengths in the Galaxy and the SMC. The non-LTE loci are for magnesium abundances of 7.58 dex (dashed) and 6.78 dex (solid) and for $v_{\rm turb} = 10\,{\rm km s}^{-1}$. The symbols are the same as those in Fig. 1, with the open and filled symbols representing Galactic and SMC supergiants, respectively.

haviour of spectral lines as a function of effective temperature. Rather than discuss the chemical species in order of their atomic number, the species least affected by chemical processing (magnesium and silicon) will be considered prior to those potentially affected by evolutionary changes (CNO). All the theoretical results discussed below will be for the mean atmospheric parameters given by the Galactic and SMC relations shown in Fig. 1. Additionally the 'normal' B-type main sequence stellar abundances estimates are taken from the work of Kilian (1992, 1994) and may vary for different lines of the same element. These were adopted, not because they are necessarily the best currently available but rather because her analysis most closely mirrors that undertaken here (see MLD for further details) and hence form a suitable comparison.

5.4.1. Magnesium

The observed and predicted linestrengths for the Mg II doublet feature at 4481 Å are shown in Fig. 4. The figure includes non-LTE loci having magnesium abundances of 7.58 (Galactic) and 6.78 dex (SMC), with $v_{\rm turb} = 10\,{\rm km\,s}^{-1}$. As was discussed by MLD, [Mg/H] = 7.58 dex (which is 0.2 dex above the 'normal' B-type star value found by Kilian) gives a good fit to the observed linestrengths in the Galactic sample. A reasonable fit to the SMC data is then achieved by adopting an underabundance of -0.8 dex relative to the galactic supergiant sample. This is in good agreement with previously published metal depletions in the SMC (e.g. Rolleston et al. 1993 give an average depletion of -0.7 dex for four main sequence B-type stars in the SMC). Additionally, the success in fitting the linestrengths with a unique abundance provides indirect evidence for the consistency of the effective temperature scale over the range, $\log T_{\rm eff}$ = 4.2 to 4.4.

5.4.2. Silicon

Fig. 5 shows observed linestrengths for Si II 4128 Å and Si III 4552 Å. The theoretical loci are for a 'normal' B-type stellar abundance of 7.28 dex and a reduced abundance of 6.78 dex. In the case of the Si III feature, predicted linestrengths are not shown above 20 000 K as this feature is not well modelled at such temperatures. No Si IV features are shown as they were not observed in sufficient SMC targets to warrant comparison.

An underabundance of -0.5 dex gives a good fit to the Si II linestrengths of the SMC sample, albeit for only seven supergiants. The Si III comparison is also reasonable, although complicated by the luminosity sensitivity of this line. For example, as the SMC sample is predominantly Ia and Iab supergiants, it shows a tight W_λ-$T_{\rm eff}$ relation, whereas the Galactic sample which containing Ib supergiants, shows more scatter. A depletion of -0.5 dex is smaller than previously reported (Dufton et al. 1990 and Rolleston et al. 1993 estimate silicon depletions of ~ -0.7 dex); however given the observational and theoretical uncertainties the difference is probably not significant.

5.4.3. Carbon

Fig. 6 shows observed and predicted linestrengths for lines of C II at 4267 and 6578 Å. Again, modelling difficulties mean that synthetic linestrengths are not given above 20 000 K for the feature at 6578 Å (see MLD for details). The non-LTE widths are computed for 'normal' carbon abundances of 7.80 dex (4267 Å) and 8.20 dex (6578 Å) and for underabundace offsets of -0.7 and -1.2 dex.

The carbon abundance in the SMC sample appears to more depleted than -0.7 dex, but there is also evidence for a partic-

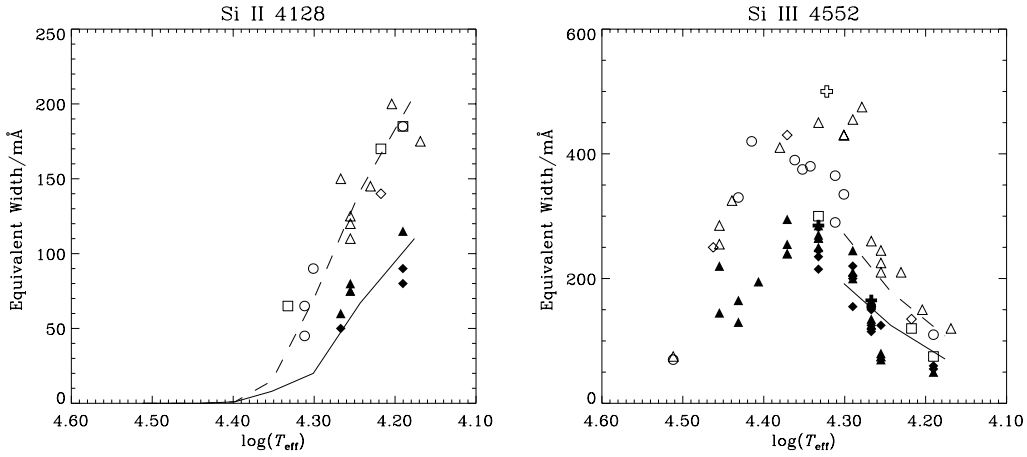

Fig. 5. Observed Si II 4128 Å and Si III 4552 Å linestrengths in the Galaxy and the SMC. The non-LTE loci are for silicon abundances of 7.28 dex (dashed) and 6.78 dex (solid) and for $v_{\rm turb} = 10\,{\rm kms}^{-1}$. The symbols are the same as those in Fig. 1, with the open and filled symbols representing Galactic and SMC supergiants, respectively.

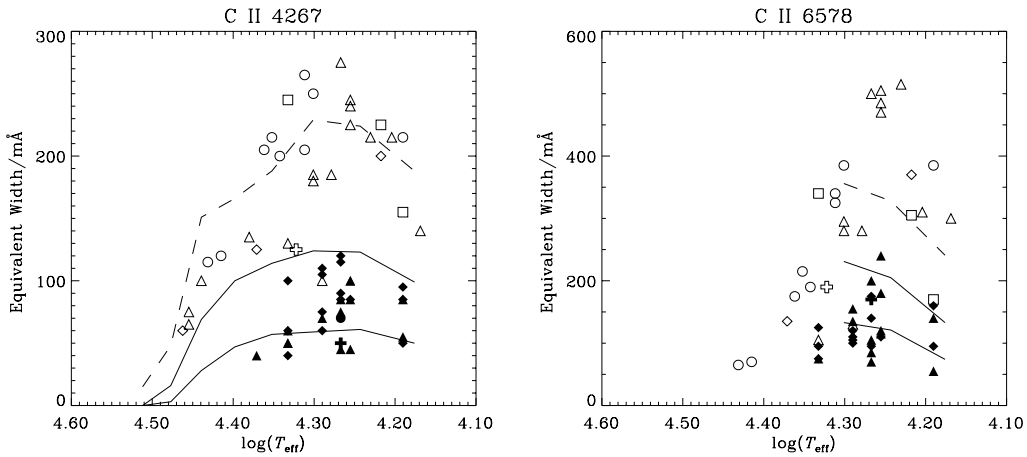

Fig. 6. Observed C II 4267 Å and 6578 Å linestrengths in the Galaxy and the SMC. The dashed non-LTE loci are for carbon abundances of 7.80 dex (for the line at 4267 Å) and 8.20 dex (6578 Å), and for relative offsets of -0.7 and -1.2 dex (solid) and for $v_{\rm turb} = 10\,{\rm kms}^{-1}$. The symbols are the same as those in Fig. 1, with the open and filled symbols representing Galactic and SMC supergiants, respectively.

ularly large spread in abundance. The former agrees with the previously published depletions in main sequence B-type stars of -0.9 dex or more (Rolleston et al. 1993 and Dufton et al. 1990). The possibility that the large spread in SMC linestrengths is related to evolutionary effects will be discussed below.

5.4.4. Nitrogen

Fig. 7 shows observed and predicted linestrengths for the N II features at 4241 & 4630 Å. These features have been selected as they are from triplets levels and appear to be more reliably modelled than singlet features, such as 3995 Å. As was discussed in MLD, the very large spread in observed N II linestrength in the Galactic sample makes it impossible to obtain a satisfactory fit with a unique abundance. The figures include loci having the 'normal' non-LTE abundance of 7.69 dex (which appears to fit the lower envelope of the Galactic sample line strengths), as well as loci with depletions of -0.2 and -0.6 dex; the latter appears to fit the lower envelope of the SMC sample line strengths.

For the SMC sample, there is again a spread in equivalent widths at a given temperature. However it is unclear whether this reflects differences in the stellar nitrogen abundances, or might be due to observational errors for these relatively weak lines and to model uncertainties – for example, variations in the microturbulent velocity. In any case, some of the SMC supergiants would appear to be depleted in nitrogen by -0.6 dex – a value which is smaller than is typically found for other young, unevolved objects in the SMC. For example the analysis of three main sequence B-type stars yielded an upper limit of ≤ -0.9 dex for nitrogen (Rolleston et al. 1993, 1999). Furthermore Russell & Dopita (1989) found nitrogen to be underabundant by -1.0 dex and -1.3 dex in H II regions and supernova remnents respectively. (~ -1.1 dex). The possible role of evolutionary effects in these lines will be discussed below.

5.4.5. Oxygen

Fig. 8 shows observed and predicted linestrengths for the O II features at 4075 and 4661 Å, with non-LTE loci for a 'normal' abundances of 8.55 and an underabundance of -0.6 dex. The assumed microturbulence of 10 km s^{-1} may be too small for this species, as the normal abundance does not provide a good fit for the strongest Galactic lines (see the discussion in MLD and Vrancken 1998). However, it would appear that an oxygen abundance of 7.95 dex gives a reasonable fit to the SMC linestrengths. The estimated depletion in main sequence objects is -0.5 dex (Rolleston et al. 1993), in reasonable agreement with the value derived here for the supergiants.

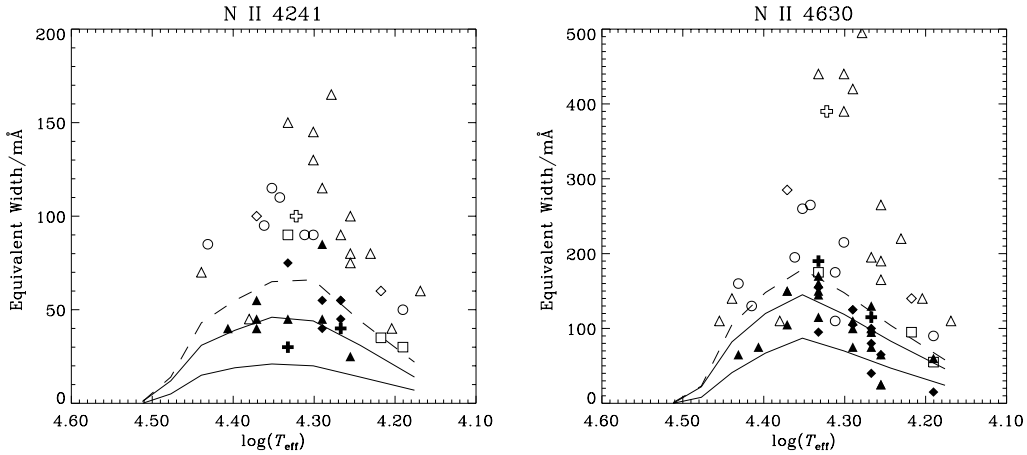

Fig. 7. Observed N II 4241 Å and 4630 Å linestrengths in the Galaxy and the SMC. The non-LTE loci are for nitrogen abundances of 7.69 dex (dashed) and for relative offsets of −0.2 and −0.6 dex (solid) and for $v_{\rm turb} = 10\,{\rm kms}^{-1}$. The symbols are the same as those in Fig. 1, with the open and filled symbols representing Galactic and SMC supergiants, respectively.

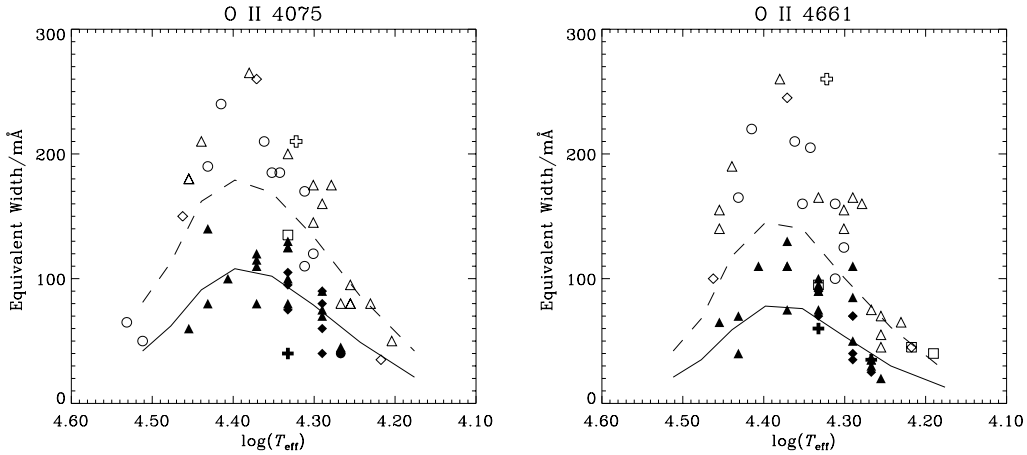

Fig. 8. Observed O II 4075 Å and 4661 Å linestrengths in the Galaxy and the SMC. The non-LTE loci are for oxygen abundances of 8.55 dex (dashed) and 7.95 dex (solid) and for $v_{\rm turb} = 10\,{\rm kms}^{-1}$. The symbols are the same as those in Fig. 1, with the open and filled symbols representing Galactic and SMC supergiants, respectively.

6. Evidence for chemical peculiarities

There were some difficulties in reproducing the linestrength patterns in the SMC supergiants. Undoubtedly, the moderate quality of the observational data, variations in the gravity and the use of a coarse effective temperature scale have exacerbated such problems. However, despite the shortcomings of the methods, reasonable fits were achieved for the helium, magnesium, and silicon lines of the SMC supergiants.

By contrast, the SMC carbon, nitrogen and oxygen line strengths could not be replicated using unique abundances - a similar effect had been previously found for the Galactic sample by MLD. They considered the linestrength ratio of N II 4630 to C II 4267 Å and found a segregation into chemically normal and processed Galactic supergiants. This procedure has been repeated for the SMC supergiants and the results are shown in Fig. 9, along with the Galactic results for reference. For clarity of presentation and to prevent congestion associated with the $T_{\rm eff}$-spectral type calibration, effective temperatures for the SMC supergiants has been multiplied by random numbers between 0.95 and 1.05.

The error bars in the SMC ratios are much larger than their Galactic counterparts due to their reduced linestrengths. Indeed there are early-type SMC supergiants whose C II or N II features could not be measured and hence some objects with apparently very large or small [N/C] linestrength ratios are not shown. These include some of the most striking examples of the OBN/OBC object class, such as AV 487 (BC0 Ia) and AV 215 (BN0 Ia) – Lennon (1997).

A theoretical [N/C] linestrength ratio has not been included in the figure, due to the uncertainties in defining representative carbon and nitrogen abundances for the SMC. Indeed, the large nitrogen depletions implied by some main sequence B-type stars (Rolleston et al. 1993) are beyond the limits of our non-LTE grids. Nevertheless, there is clearly a very large range in observed N/C linestrength ratios in the SMC supergiant sample, larger even than in the Galactic case (particularly when the SMC supergiants excluded from the plot are considered). It is possible that the non-LTE locus for a normal SMC N/C abundance ratio would lie close to the normal Galactic locus, which would mean that some of the SMC sample show evidence for chemical evolutionary effects. Alternatively, the nitrogen depletion deduced for the SMC supergiants appeared to be less than that for main sequence targets (see Sect. 4.3.4) and hence it is possible that the whole SMC supergiant sample is nitrogen enriched.

Investigations by other authors of CNO abundances from luminous stars in the Magellanic Clouds could provide a useful baseline for comparison with the current sample. The evidence on CNO abundances found by Venn (1999) for A-type super-

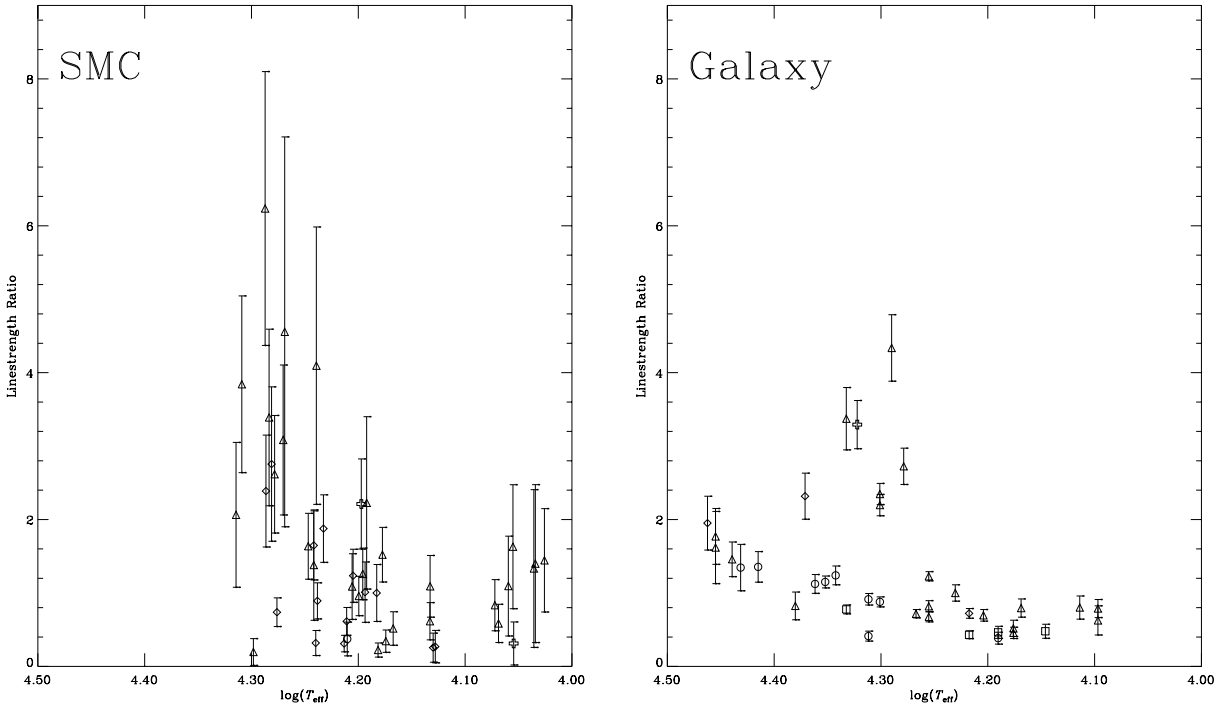

Fig. 9. Oberved equivalent width ratios for the lines at 4630 Å (N II) and 4267 Å (C II) for the SMC and Galactic supergiants. The error bars reflect uncertainties in the linestrength measurements. Note that those SMC supergiants for which one or both of the features were not measured are not plotted. The symbols represent different luminosity classes and are the same as in Fig. 1.

giants, that of Luck & Lambert (1992), Russell & Bessell (1989) and Spite et al. (1989) for F-type supergiants, and that of Hill et al. (1997) for K-type supergiants is relevant as B-type supergiants may be progenitors (or, indeed, descendants) of such objects. Also, the work on main sequence objects (Dufton et al. 1990, Rolleston et al. 1993) may provide estimates for the unprocessed abundances. However, until better quality observational data are obtained, any comparisons with such work would be premature. Indeed we are currently obtaining high quality echelle spectroscopy with the Anglo-Australian telescope for a subset of our SMC targets in order to address these problems.

7. Conclusions

We emphasize that the current study must be considered as exploratory, given the quality of the observational data and the uncertainties in the atmospheric parameters. However, our principle conclusions are as follows.

1. The atmospheric parameters for the SMC supergiants are similar to those found for the Galactic sample of MLD. Additionally the range of luminosities (and hence of inferred masses) are similar in the two samples.
2. The helium abundances in the SMC supergiants are similar to those for the Galactic sample and are in general compatible with the value found for main sequence stars.
3. The underabundances of magnesium and silicon in the SMC supergiants (compared with their Galactic counterparts) are consistent with values previously found for SMC objects.
4. The carbon, nitrogen and oxygen line strengths imply a range of abundances, with the variation in the C/N abundance ratio in the SMC supergiants appearing to be at least as large as in their Galactic couterparts.

Acknowledgements. We would like to thank Rolf Kudritzki, Kim Venn, Norbert Langer and Robert Rolleston for many useful discussions. This work has made use of model atmosphere programs made available through the PPARC supported Collaborative Computational Project No. 7. NDME would like to acknowledge financial support from the Department of Education for Northern Ireland, while DJL is grateful for support from the Bundesminister für Forschung und Technologie under grant 010 R 90080. We are grateful to the British Council and the Akademischer Austauschdienst for funding an ARC program of working visits between Munich and Belfast.

References

Azzopardi M., Vigneau J., 1982, A&AS 50, 291
Becker S.R., Butler K., 1988, A&A 201, 232
Becker S.R., Butler K., 1989, A&A 209, 244
Becker S.R., Butler K., 1990, A&A 235, 326
Butler K., 1984, Ph.D. Thesis, University of London
Denissenkov P., 1994, A&A 287, 113
Dufton P.L., Fitzsimmons A., Howarth I.D., 1990, A&A 362, L59
Fitzpatrick E.L., 1988, ApJ 335, 703
Fitzpatrick E.L., Garmany C.D., 1990, ApJ 363, 119
Fransson C., Cassatella A., Gilmozzi R., et al., 1989, ApJ 336, 429
Gabler R., Gabler A., Kudritzki R.-P., Puls J., Pauldrach A., 1989, A&A 226, 162
Garmany C.D., Conti P.S., Massey P., 1987, AJ 93, 1070
Giddings J.R. 1981, Ph.D. Thesis, University of London

Hill V., 1998, In: Chu Y.H., Subtzeff N. (eds.) New Views on the Magellanic Clouds. ASP Conf Series, p. 19
Hill V., Barbuy B., Spite M., 1997, A&A 323, 461
Hubeny I., 1988, Computer Physics Comm. 52, 103
Humphreys R.M., 1983, ApJ 265, 176
Kilian J., 1992, A&A 262, 171
Kilian J., 1994, A&A 282, 867
Kurucz R.L., 1991, In: Davis-Philip A.G., Upgren A.R., Janes P.L. (eds.) Precision Photometry: Astrophysics of the Galaxy. L. Davis Press, Schenectady, p. 27
Lamers H.J.G.L.M., 1981, ApJ 245, 593
Langer N., Heger A., 1998, In: Howarth I.D. (ed.) Boulder-Munich II: Properties of hot, luminous stars. ASP Conf. Ser. 131, 76
Langer N., Maeder A., 1995, A&A 295, 685
Langer N., Heger A., Braun H., 1999, Nucleosynthesis in Massive stars. In: Mezzacappa T. (ed.) Atomic and Nuclear Astrophysics: Proc. 2nd. Oak Ridge Symposium, IOP publishing, p. 377
Lennon D.J., 1997, A&A 317, 871
Lennon D.J., Dufton P.L., Mazzali P.A., Pasian F., Marconi G., 1996, A&A 314, 243
Lester J.B., Gray R.O., Kurucz R.L., 1986, ApJS 61, 509
Luck R.E., Lambert D.L., 1992, ApJS 79, 303
Maeder A., Meynet G., 1989, A&A 210, 155
Massey P., Lang C.C., de Gioia-Eastwood K., Garmany C.D., 1995, ApJ 438, 188
McErlean N.D., Lennon D.J., Dufton P.L., 1999, A&A in press (MLD)
Meynet G., 1998, In: Howarth I.D. (ed.) Boulder-Munich II: Properties of hot, luminous stars. ASP Conf. Ser. 131, p. 96
Rolleston W.R.J., Dufton P.L., Fitzsimmons A., Howarth I.D., Irwin M.J. 1993, A&A 277, 10
Rolleston W.R.J., Brown P.J.F., Dufton P.L., Howarth I.D., 1996, A&A 315, 95
Rolleston W.R.J., Hambly N.C., Dufton P.L., et al., 1997, MNRAS 290, 422
Rolleston W.R.J., Dufton P.L., McErlean N.D., Venn K.A., 1999, A&A 348, 728
Russell S.C., Bessell M.S., 1989, ApJS 70, 865
Russell S.C., Dopita M.A., 1989, ApJ 384, 508
Schaller G., Schaerer D., Meynet G., Maeder A., 1992, A&AS 96, 269
Sanduleak N., 1968, AJ 73, 246
Spite M., Barbuy B., Spite F., 1989, A&A 222, 35
Talon S., Zahn J.-P., Maeder A., Meynet G., 1997, A&A 322, 209
Venn K.A., 1995a, ApJS 99, 659
Venn K.A., 1995b, ApJ 449, 839
Venn K.A., 1999, ApJ in press
Venn K.A., McCarthy J.K., Lennon D.J., Kudritzki R.-P., 1998, In: Howarth I.D. (ed.) Boulder-Munich II: Properties of hot, luminous stars. ASP Conf. Ser. 131, p. 108
Voels S.A., Bohannan B., Abbott D.C., Hummer D.G., 1989, ApJ 340, 1073
Vrancken M., 1998, Ph.D. Thesis, Vrije Universiteit Brussel
Walborn N.R., 1977, ApJ 215, 53
Walborn N.R., 1983, ApJ 265, 716